Layer-by-layer growth of sodium chloride overlayers on an Fe(001)-p(1 × 1)O surface

2012 Nanotechnology 23 505602

(http://iopscience.iop.org/0957-4484/23/50/505602)

Nanotechnology **23** (2012) 505602 (8pp) doi:10.1088/0957-4484/23/50/505602

Layer-by-layer growth of sodium chloride overlayers on an Fe(001)-p(1 × 1)O surface

Antoni Tekiel, Jessica Topple, Yoichi Miyahara and Peter Grütter

Physics Department, McGill University, 3600 University Street, Montreal, QC H3A 2T8, Canada

E-mail: antoni.tekiel@mail.mcgill.ca

Received 27 August 2012, in final form 28 October 2012
Published 27 November 2012
Online at stacks.iop.org/Nano/23/505602

Abstract
Ultra-thin NaCl films epitaxially grown on an Fe(001)-p(1 × 1)O surface have been investigated in ultra-high vacuum by non-contact atomic force microscopy and low energy electron diffraction. It has been found that at temperatures below 145 °C NaCl initially grows as monoatomic thick islands on substrate terraces, while at temperatures above 175 °C biatomic thick islands are also formed at substrate step edges. Both types of islands have the same Fe(001)–O[100] ‖ NaCl(001)[110] orientation, leading to a (4 × 4) superstructure, where the NaCl unit cell is oriented at 45° with respect to the substrate. Interestingly, no c(2 × 2) superstructure with the NaCl unit cell oriented at 0° has been observed. The oxygen on the iron surface promotes layer-by-layer growth, resulting in atomically flat films with 40–60 nm wide terraces at coverages ranging from 0.75 to 12 ML. Such NaCl films are of much higher quality than MgO films grown on Fe(001) and Fe(001)-p(1 × 1)O surfaces and represent a unique epitaxial system of an alkali halide on a pure metallic substrate. The reduced number of defects and the layer-by-layer mode of growth make this system very attractive for applications where an atomically defined tunnel barrier is required to control the properties of a device.

(Some figures may appear in colour only in the online journal)

1. Introduction

Crystalline insulating ultra-thin films grown on a variety of metallic and semiconducting substrates attract considerable attention because of their importance in magnetoelectronics [1] and catalysis [2]. They are frequently used in systems where the film serves as a tunnel barrier directly controlling the properties of a device. For example, in magnetoelectronic applications and in model systems for heterogeneous catalysis the insulating film is often made of magnesium oxide that can be grown epitaxially layer by layer, usually on (001) surfaces of various metals, allowing for control of the tunnel barrier thickness. For this reason there has been recently stimulated interest in the growth and properties of crystalline oxide thin films [3], which includes oxides such as MgO, Al_2O_3, TiO_2 and V_2O_3. However, fully crystalline oxide thin layers are difficult to grow and are usually oxygen deficient. In the case of MgO films, these difficulties have been attributed to the MgO-metal lattice mismatch and the fact that in ultra-high vacuum (UHV), regardless of the preparation method, MgO is essentially grown from two separate sources of magnesium and oxygen, which have to react on the substrate to nucleate an the MgO molecule [4, 5]. The quality of such oxide films is still much lower than that of insulating films based on alkali halides that, especially on closely lattice matched AIII-BV compound semiconductors, can form well-ordered films [6]. This quality difference can be explained by the fact that alkali halides, such as NaCl and KBr, evaporated thermally form predominantly molecular dimers, and thus their growth is much better controlled due to the reduced complexity of on-surface nucleation.

Recent band structure calculations by Vlaic [7] predicted a high tunnel magnetoresistance (TMR) ratio for Fe/NaCl/Fe(001) magnetic tunnel junctions (MTJs), but the

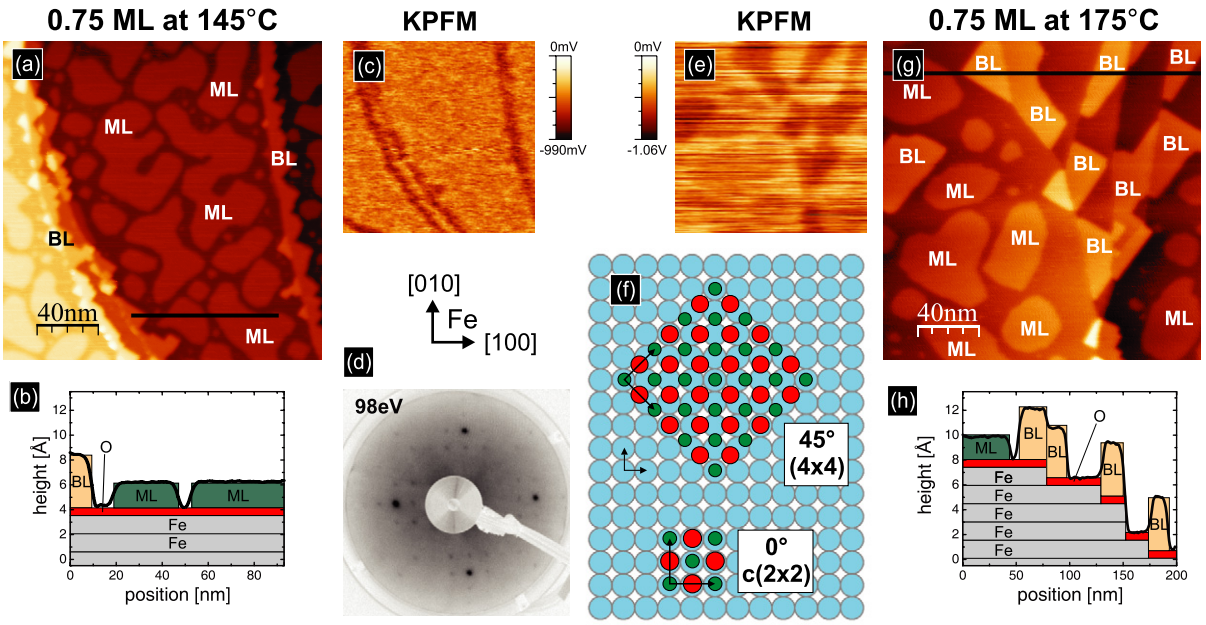

Figure 1. The structure of 0.75 ML NaCl film on Fe(001)-p(1 × 1)O grown at 145 °C and 175 °C. (a) and (g) NC-AFM topography images, (c) and (e) KPFM images, (b) and (h) typical cross sections and schematic coverage models for growth at 145 °C and 175 °C, respectively. (d) LEED image of 0.75 ML NaCl film grown on Fe(001)-p(1 × 1)O at 145 °C taken at the electron energy of 98 eV. (f) Schematic representation of the NaCl film in both considered configurations.

experimental realization of such devices has been unsuccessful due to difficulties in sample preparation [8]. The growth of NaCl on iron is difficult to improve, probably because of corrosion of the substrate by NaCl during deposition or annealing of the system at elevated temperatures. Moreover, the closely matched lattices of NaCl and Fe in the c(2 × 2) structure do not necessarily have to lead to good epitaxy. For example, on the *fcc* Ag(001) surface, where a NaCl film compressed by 2.7% could form a (4 × 4) structure, the growth is incommensurate with significant mosaic spread [9], and this also leads to other orientations. More importantly the NaCl does not wet the silver surface, leading to a 3D growth starting even from the first layers.

The chemical and elastic properties of the Fe(001) surface, which strongly influence the growth of NaCl films, can be easily modified by terminating the surface with chemisorbed oxygen atoms. Exposure to several Langmuir of oxygen followed by flash annealing gives rise to the well-known Fe(001)-p(1 × 1)O surface, which has been thoroughly investigated by experimental and computational methods [10, 11]. The surface is characterized by one oxygen atom per unit cell chemisorbed in each hollow site of the Fe(001) and the same lattice parameter as the Fe(001) surface. As will be discussed in this work, the chemisorbed oxygen layer likely prevents the Fe(001) surface from a reaction with NaCl. Higher chemical stability allows for the use of elevated temperatures during sample preparation to enhance the diffusion of NaCl and improve the film quality. Moreover, the top layer of the Fe(001)-p(1 × 1)O surface resembles a planar rocksalt FeO monolayer. Compared to clean bulk iron, rocksalt FeO has a higher compliance, due to which the Fe(001)-p(1 × 1)O surface acts as a strain buffer in the epitaxy of thin films on top of it [12].

In this work, we report on layer-by-layer growth of well-ordered, ultra-thin NaCl films on an oxygen covered Fe(001) surface. High-resolution non-contact atomic force microscopy (NC-AFM) measurements reveal that NaCl forms films of quality much higher than MgO on Fe(001), a prototype system among single-crystal MTJs. Although alkali halide films have been successfully grown on semiconductor surfaces with comparable quality, there has been no report on a layer-by-layer growth of alkali halide films on a purely metallic substrate. The cubic lattice constant of *bcc* iron differs only by 1.8% from the nearest neighbor distance of the NaCl crystal, which should favor growth of a stretched NaCl film with a c(2 × 2) symmetry and its unit cell oriented at 0° with respect to that of the Fe(001), as shown in figure 1(f). We show, however, that this is not the case, and that the NaCl film is orientated at 45° with a (4 × 4) symmetry, which leads to a compression of the film by 4.2%. This unexpected film orientation is rationalized by the fact that an unsupported NaCl monolayer has a smaller lattice parameter than bulk NaCl, as the Madelung constant is reduced for a 2D ionic crystal. Consequently, with the NaCl unit cell orientated at 45°, the first NaCl monolayer is almost perfectly matched with the Fe(001)-p(1 × 1)O substrate in the (4 × 4) configuration.

2. Methods

All experiments reported here are performed in two interconnected UHV chambers (preparation and microscope) based on a commercial JEOL JSPM 4500a UHV AFM

system. The base pressure is in the low 10^{-11} mbar range in the preparation and 1×10^{-10} mbar in the microscope chamber. Iron whiskers home grown by reduction of $FeCl_2$ in an H_2 atmosphere with {001} side-surface orientations are used as the starting substrate [13]. The whiskers are cleaned by several cycles of 1 keV Ar^+ bombardment and subsequent annealing to about 600 °C until a clean low energy electron diffraction (LEED) pattern is observed, which leads to a surface with terraces several hundred nanometers wide. To produce the Fe(001)-p(1 × 1)O surface, the clean iron substrate is exposed to 8 L of molecular oxygen (99.997% purity) at room temperature and subsequently annealed to 400 °C to remove the excess oxygen. A piece of NaCl single crystal (Korth Kristalle GmbH) is outgassed in vacuum and evaporated from a Knudsen cell onto the Fe(001)-p(1 × 1)O sample kept at temperatures in the 90–250 °C range. Non-contact atomic force microscopy is carried out at room temperature in the frequency modulation (FM) mode using a JEOL AFM and Nanosurf 'easyPLL' frequency detector. Commercial Nanosensors PPP-NCLR silicon cantilevers with a typical resonance frequency of 150–160 kHz and spring constant of ≈42 Nm^{-1} are used with an oscillation amplitude of 5–7 nm. Two FM NC-AFM imaging modes are used. In the first one, used to record most of the images here, the frequency shift of the cantilever is maintained constant by a feedback loop controlling the *z*-piezo position, which is called the 'topography mode'. The second mode, called the 'quasi-constant-height mode', used for obtaining atomic resolution, acquires the image with the feedback loop set to a very low value. In this case a frequency shift map is measured where brighter levels indicate larger negative frequency shifts. In the topography mode simultaneous FM Kelvin Probe Force Microscopy (KPFM) (with 800 Hz modulation frequency and $V_{RMS} = 800$ mV modulation amplitude) is used to compensate for the local contact potential difference (LCPD) [14]. LEED images are taken with the use of four-grid LEED optics (Specs ErLEED).

3. Results and discussion

3.1. NaCl adsorption on Fe(001)-p(1 × 1)O at submonolayer coverage

Submonolayer coverage of NaCl (approximately 0.75 ML; one monolayer is defined as a one-atom-thick layer) is deposited at various sample temperatures and characterized by NC-AFM and KPFM (figure 1). As shown in figure 1(a) at temperatures of 145 °C and below, NaCl nucleates predominantly on the terraces and forms interconnected monolayer islands (measured height of 1.9 Å—see figure 1(b)) that are roughly square shaped showing preferential alignment of edges with ⟨110⟩ directions of the substrate. There is also some nucleation of NaCl bilayers (measured height 4.2 Å) at the step edges of the Fe(001)-p(1 × 1)O surface. If the substrate temperature during the growth is increased to 175 °C and above, the nucleation at the step edges becomes more pronounced and both types of islands are larger, as shown in figure 1(g). The same monolayer islands as described for the growth at lower temperatures form on the terraces and bilayer islands nucleate at the step edges. Sporadically bilayer islands nucleated on a terrace can be found. The KPFM images (shown in figures 1(c) and (e)) show weak contrast between the uncovered Fe(001)-p(1 × 1)O surface and the first NaCl monolayer. However, there is significant LCPD observed for Fe(001)-p(1 × 1)O and NaCl bilayers, indicating a work function difference of ≈1 eV. A similar trend in the LCPD dependence on the NaCl coverage has been described by Prada *et al* for various insulating overlayers on metallic substrates [15].

The alignment of the edges of monolayer NaCl islands indicates that the unit cell of NaCl is rotated by 45° with respect to the substrate unit cell (see figure 1(f)). In this orientation, the (4 × 4) structure can be identified as the most probable higher-order commensurable NaCl relationship with the film compressed by 4.2%. This prediction is confirmed by an experimental LEED pattern shown in figure 1(d) of a 0.75 ML thick NaCl film grown on Fe(001)-p(1 × 1)O at 145 °C, with not only first-order diffraction spots visible for the Fe(001) surface and the NaCl film, but also a clear (4 × 4) superstructure that is due to the formation of a new, four times larger, unit cell at the NaCl/Fe(001)-p(1 × 1)O interface.

So far we have used the bulk lattice parameter for discussion of epitaxial relationship in the growth of NaCl films on the Fe(001)-p(1 × 1)O surface. However, even a simple approximation based on Madelung energy (explained in the appendix) shows that an NaCl monolayer with a {001} orientation favors a smaller distance between closest Na^+ and Cl^- ions of 5.36 Å, which compared to 5.64 Å for bulk NaCl is reduced by 4.7%. More accurate calculations based on density functional theory (DFT) have provided similar values: 5.40 Å [16], 5.45 Å [17] and 5.55 Å [18]. The matched lattice parameters of the NaCl monolayer in the (4 × 4) and c(2 × 2) structures are 5.41 Å and 5.74 Å, respectively. Using the same approach based on Madelung energy, one can estimate the energy cost for stretching an unsupported monolayer to match the (4 × 4) and c(2 × 2) surface lattices of Fe(001), which gives only 0.0027 eV for the former, but 0.1114 eV for the latter (per one NaCl molecule). This difference in energy cost suggests that formation of the c(2 × 2) structure would require much larger site-dependent film–substrate interaction, while the lattice of an NaCl monolayer is almost perfectly matched in the (4 × 4) configuration.

3.2. Structure of 2 ML thick NaCl film

Figure 2 shows the influence of substrate temperature during deposition on the morphology of NaCl film that has a nominal thickness of 2 ML. When deposited at 120 °C the surface is mostly uniformly covered with NaCl film with a small number of holes in it and a few islands in the third atomic layer (figure 2(a)), revealing a layer-by-layer growth with a small amount of roughening. If the substrate temperature is higher during the growth (145 °C and above—see figures 2(b) and (c)), the growth at substrate step edges starts to disturb the nearby growth. The islands next to step edges are usually

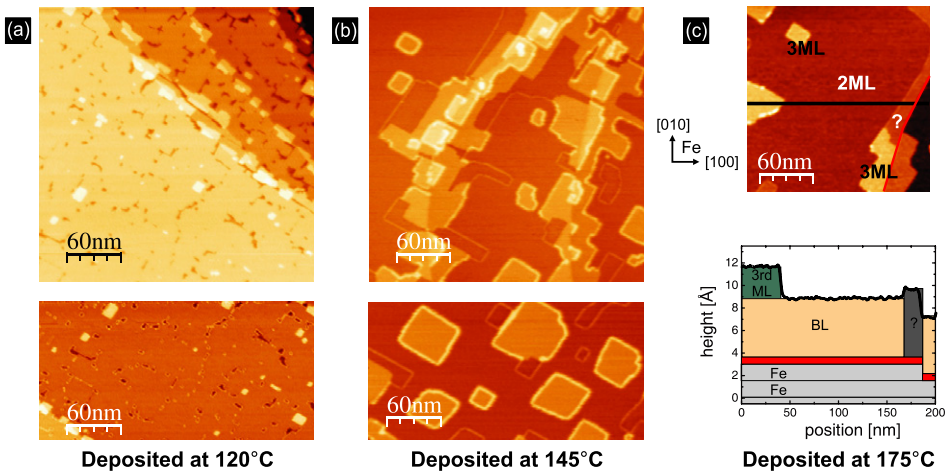

Figure 2. Structure of 2 ML NaCl film on Fe(001)-p(1 × 1)O grown at (a) 120 °C, (b) 145 °C and (c) 175 °C. (a) and (b) show well-defined irregular networks of dislocations that appear as bright lines and far from step edges usually align along ⟨110⟩ directions of the substrate. (c) Typical cross section taken above an underlying Fe step edge and schematic coverage model for growth at 175 °C. The red line in the NC-AFM image shows the position of the substrate step edge.

taller than the NaCl film on average, and there is a distinct, irregular network of dislocations, especially nearby such areas that locally are covered by a larger number of atomic NaCl layers. As clearly shown in figure 2(b), on the terraces, such dislocations appear as bright lines in the AFM image and far from step edges usually run along ⟨110⟩ directions of the substrate (one should distinguish these bright dislocation lines from NaCl step edges which also appear as bright lines in figure 2(b), a common contrast in imaging alkali halides films by NC-AFM [19]). The cross section in figure 2(c) shows that close to the step edges, where the film morphology is irregular (which happens especially after the deposition at temperatures above 145 °C) the height of the NaCl film in some regions cannot be assigned to any integral number of monolayers, indicating that the local orientation of the film may differ. Based on the DFT calculations by Olsson *et al* [18], although an unsupported NaCl monolayer is characterized by a much smaller lattice parameter, already an NaCl bilayer has a lattice parameter similar to the bulk value. This means that in the 2 ML coverage range the NaCl film experiences a significant change in energetically favorable distance between closest Na^+ and Cl^- ions. Therefore, the well-defined bright lines, which are observed on all 2 ML samples grown at temperatures 120–175 °C, can be identified as a mechanism of strain relief due to overgrowing of the first by the second NaCl monolayer and related to structural instabilities of the film. It should be noted that considering only the almost bulk-like lattice parameter of a 2 ML thick unsupported film, the NaCl film could be better matched with the Fe(001)-p(1 × 1)O substrate in the c(2 × 2) orientation. However, this simple picture does not correspond to the real process of the film growth and the first monolayer determines the orientation of the film, regardless of how many subsequent layers are deposited.

3.3. Structure of 4 ML thick NaCl film: effect of post-annealing

Figure 3(a) shows NaCl coverage of nominal 4 ML deposited at 120 °C, where a completed third ML, incomplete fourth ML and a very small number of islands in 5th ML are visible. The islands in the fourth ML have typical size of 30–50 nm across. One cannot observe dislocation lines that are characteristic for the structure of 2 ML thick film, which suggests that layers beyond the first 2 ML overgrow successfully the interface with such defects. Although the topography in figure 3(a) reveals only a very well-ordered incomplete 4 ML thick film, the LCPD map recorded on the as-deposited sample (figure 3(b)) shows a complex pattern with significant local variations (68% values are within an interval of 148 mV). Such local changes in LCPD indicate that the film is nonuniform and because the top-most layer is near perfect and the only defects can be attributed to step edges due to an incomplete fourth ML, this variation must originate from subsurface structural defects in the deeper lying layers of the NaCl film. In figure 3(c) the positions of islands edges from the fourth ML are superimposed with the KPFM image. The dark spots are usually located within central areas of the islands of the fourth ML, which means that the position of the defects and the distribution of those islands are mutually correlated.

Figures 3(d) and (e) show the change after annealing at 160 °C in the sample morphology and LCPD, respectively. The sample is similarly characterized by a network of coalesced islands that have become larger on average. It is worth noting that the NaCl coverage remains similar and there is no noticeable reevaporation of NaCl from the surface. Interestingly, after annealing the LCPD contrast is more uniform (68% values are within an interval of 84 mV), but more importantly it does not have the same feature pattern observed prior to annealing. This suggests that the subsurface defects in the NaCl film have been partly healed and now have less impact on the film morphology and strain. Figure 3(f) also

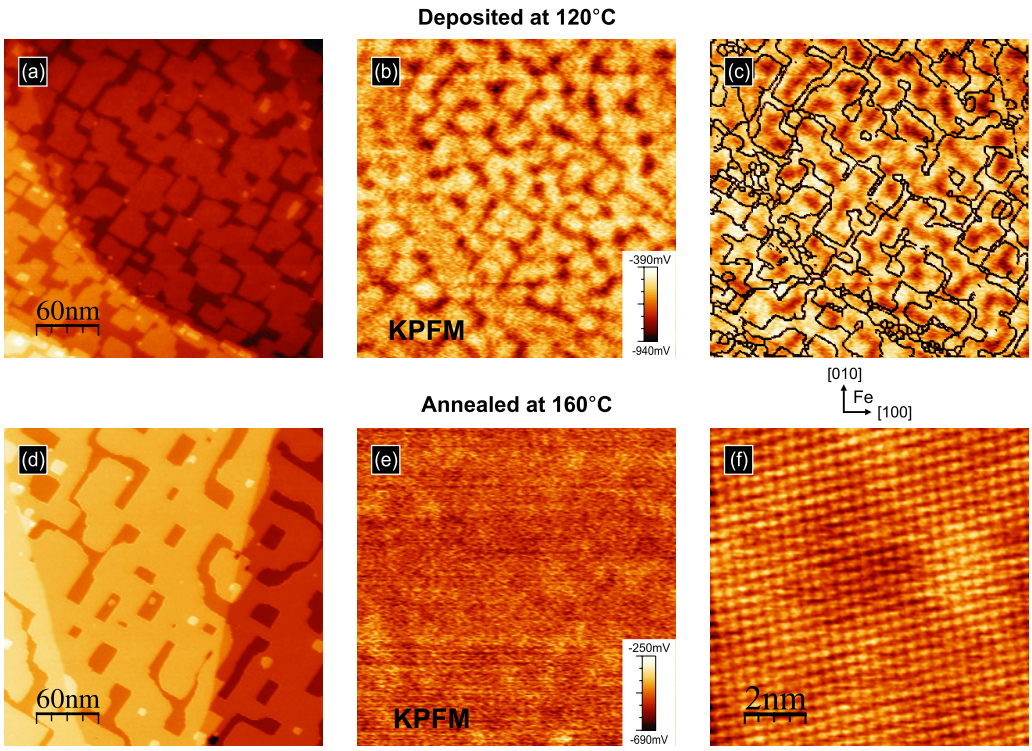

Figure 3. Structure of 4 ML NaCl film on Fe(001)-p(1 × 1)O grown at 120 °C and after additional post-annealing at 160 °C. (a) and (d) NC-AFM topography images, (b) and (e) KPFM images for as-grown samples and after post-annealing, respectively. (b) A nonuniform LCPD map recorded on the as-deposited sample with significant local variations. (c) The positions of island edges from (a) superimposed on the KPFM image (b) showing that dark spots in LCPD are usually located within central areas of the islands of the fourth ML. (e) KPFM image after post-annealing showing a more uniform LCPD pattern without features correlated with positions of NaCl islands. (f) Molecularly resolved image (the lattice is slightly distorted due to thermal drift) confirming that the NaCl unit cell is oriented at 45°, as expected in the (4 × 4) structure.

shows a molecularly resolved image (i.e. either the Na or the Cl sublattice, marked by green or red in figure 1(f)) of the fourth ML, confirming independently that the NaCl unit cell is oriented at 45° with respect to the unit cell of the substrate, as expected for the (4 × 4) structure.

3.4. Layer-by-layer growth

Starting from the second ML, the NaCl film successfully overgrows the Fe(001)-p(1 × 1)O step edges, which proves that this system can be used to fabricate continuous and uniform tunnel barriers over large sample areas that exceed the typical size of Fe(001)-p(1 × 1)O terraces. Based on the above observations, we propose a protocol to fabricate high quality NaCl films, where the film is first grown at a temperature hindering the extended growth at the step edges (120 °C), and next it is annealed at higher temperature (160 °C for 2 h) to improve the crystallinity and increase the average island size. Figure 4 shows an example of almost layer-by-layer growth of 12 ML thick NaCl film. Although the height of a step edge on the Fe(001)-p(1 × 1)O surface is 1.44 Å, which does not match the distance between the atomic planes in the NaCl crystal, the NaCl still overgrows the substrate step edges. The inset in figure 4 shows positions of substrate step edges of atomic height. In such cases only screw dislocations on top of the step edges form and the average coverage of the film is preserved. This proposed protocol is potentially useful for application in nanoscale systems requiring continuous and uniform crystalline tunnel barriers, including magnetoelectronic and catalytic applications, but also in fundamental science where ultra-thin films are frequently used to decouple electronically adsorbates from the metallic substrate [20]. NaCl films can be grown on the Fe(001)-p(1 × 1)O surface layer by layer with a remarkable quality up to a thickness of 12 ML, as demonstrated in this work.

3.5. The role of oxygen

The role of oxygen on the growth of NaCl is significantly different to that on the growth of easily oxidizable metals. In the growth of metals on the Fe(001)-p(1 × 1)O surface, such as Mn, Cr and also the homoepitaxy of iron, oxygen acts as a surfactant and is floating during the growth on top of the deposited film, thus improving layer-by-layer growth [21]. In contrast, the interaction between oxygen and NaCl is much weaker [22] than the interaction between oxygen atoms and the Fe(001) surface, which was calculated by Blonski [23] and is characterized by adsorption energy of 3.09 eV, indicating strong chemisorption. Thus, oxygen is permanently bound to the iron surface and does not leave it, even with the NaCl film grown on top of it. Strong binding of oxygen to iron can additionally help in protecting

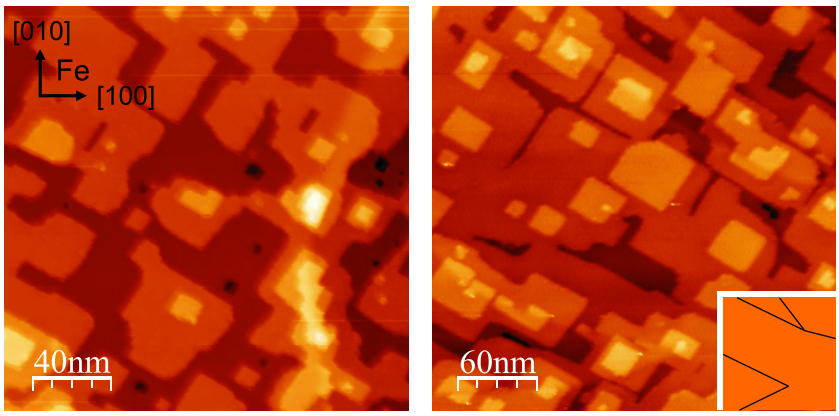

Figure 4. Structure of 12 ML NaCl film on Fe(001)-p(1 × 1)O grown at 120 °C and annealed at 160 °C for 2 h showing almost layer-by-layer growth with a small number of defects. Usually only screw dislocations on top of the substrate step edges can be observed. The inset shows the positions of substrate step edges of atomic height.

it from unwanted reaction with NaCl and formation of surface iron chloride that could be triggered at higher sample temperatures [24]. Indeed, our preliminary tests indicated that evaporation of NaCl directly onto clean Fe(001) surface even at 160 °C leads to its partial destruction. The effect of this reaction can be minimized by limiting the sample temperature during preparation, which also reduces diffusion of NaCl and the average size of NaCl islands. Figure 5 compares the morphology of 4 ML NaCl deposited at 90 °C directly onto a clean Fe(001) surface and the Fe(001)-p(1 × 1)O surface. There are two unwanted phenomena occurring on the Fe(001) surface. First, one can immediately notice that the growth on the clean Fe(001) substrate resembles the Stranski–Krastanov mode (figure 5(a)). Second, instead of only one film orientation, there are two coexisting orientations on the sample, corresponding to the (4 × 4) and c(2 × 2) structures. Sodium chloride on the Fe(001)-p(1 × 1)O surface grows layer by layer (figure 5(b), also know as Frank–van der Merwe mode), which can only be observed if there is no substantial strain in the grown film. As mentioned before, the FeO-like top layer of the substrate is expected to have a higher compliance suited to supporting thin films and acting as a strain buffer, which is clearly demonstrated in figure 5.

Calculations have shown that MTJs based on the Fe(001)/MgO/Fe(001) structure should have very high TMR ratio [25, 26], but there is a large discrepancy between the theoretical and reported experimental TMR values [27, 28]. Therefore, specific studies have focused on the role played by oxygen at the Fe/MgO interface, as this kind of contamination may easily originate from rest gases in the growth chamber or from the growth of MgO itself. It has been shown that the theoretical predictions of TMR are very sensitive to the quality of the Fe/MgO/Fe junctions. A small amount of oxygen has a drastic effect on the TMR amplitude [29, 30]. Also the oxygen deficiency of the MgO film and formation of oxygen vacancies induces detrimental diffusive scattering [31]. Additionally, MgO films on Fe(001) are characterized by a dense network of misfit dislocations, which has not yet been included in theoretical calculations. From this point of view, development of new MTJs based on crystalline NaCl ultra-thin films of much higher quality can be an alternative to MgO tunnel barriers. Moreover, such a highly ordered NaCl tunnel barrier will resolve the discrepancy between theoretical modeling and the experimental realization of a potential device.

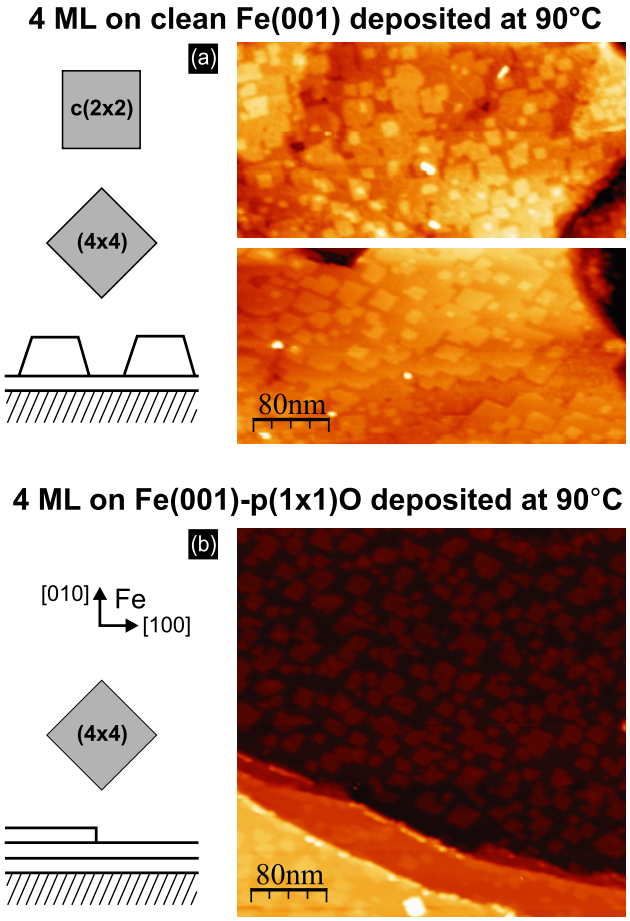

Figure 5. Comparison of the morphology of 4 ML NaCl film deposited at 90 °C directly onto (a) clean Fe(001) surface and (b) the Fe(001)-p(1 × 1)O surface. In (a) the growth resembles the Stranski–Krastanov mode and one can observe areas on the sample with film orientations corresponding to the (4 × 4) and c(2 × 2) structures. In (b) NaCl grows layer by layer, leading only to the (4 × 4) orientation.

Concerning magnetic applications of the NaCl/Fe(001)-p(1 × 1)O system, we demonstrated in this work that the formation of a FeO-like interface is crucial for obtaining layer-by-layer growth. Such high quality of ultra-thin films has never been observed in the MgO/Fe(001) system [32, 33]. Although the presence of oxygen at the interface may reduce the TMR ratio in an MTJ based on NaCl, the NaCl/Fe(001)-p(1 × 1)O system represents much higher structural quality than that of MgO films. Electronic band structure calculations [7] predicted a very high TMR ratio for the Fe/NaCl/Fe(001) MTJ (without oxygen at the interface) where the NaCl film forms the c(2 × 2) structure. Theoretical modeling is needed here to calculate the magnetic properties of (4 × 4) NaCl films on the Fe(001)-p(1 × 1)O surface and understand the impact of oxygen on the performance of a potential MTJ. Although the TMR ratio may be reduced by the presence of oxygen, the fact that the system quality is very high can be very beneficial for obtaining a high TMR ratio, as the density of states in such device may be less affected by any structural defects at the NaCl/Fe(001)-p(1 × 1)O interface.

4. Conclusions

We report a protocol for the layer-by-layer growth of well-ordered, ultra-thin NaCl films on an Fe(001)-p(1 × 1)O surface at coverages ranging from 0.75 to 12 ML. Characterization of a submonolayer reveals two growth modes: on the terraces as monoatomic thick islands and at the step edges as bilayer islands. In both cases the NaCl unit cell is oriented at 45° with respect to the substrate leading to a (4 × 4) superstructure. The effect of sample temperature during the growth and during post-annealing is identified: first, deposition at lower sample temperatures (120 °C) can successfully reduce the extended growth of bilayer islands at substrate step edges. Second, subsequent post-annealing can improve the crystallinity of the film and increase the size of NaCl terraces. We explain the (4 × 4) structure of the NaCl film by the fact that at the initial stage of growth, during formation of the first monolayer, the lattice parameter of the 2D NaCl film is reduced compared to the bulk value and in that configuration matches perfectly the Fe(001)-p(1 × 1)O lattice. The oxygen on the iron surface promotes layer-by-layer growth, allowing the formation of atomically flat films with 40–60 nm wide terraces at coverages up to 12 ML. Such high quality of NaCl films makes this system a better candidate than MgO films on metals for applications where an atomically defined tunnel barrier is needed.

Acknowledgments

We acknowledge helpful discussions with Dr Dongping Liu and Professor Hong Guo from McGill University. This work was partly supported by the Natural Sciences and Engineering Research Council (NSERC), Canadian Institute for Advanced Research (CIfAR) and Regroupement Québécois sur les Matériaux de Pointe (RQMP). AT gratefully acknowledges NSERC for financial support as a Vanier Canada Graduate Scholar.

Appendix. Lattice parameter of an unsupported NaCl monolayer

The structure of ionic crystals can be characterized by a simple model that includes the repulsion energy between the closest neighbors and the Madelung energy of the crystal lattice [34]:

$$U_{\mathrm{tot}} = N\left[z\lambda \exp\left(-\frac{R}{\rho}\right) - \alpha\frac{q^2}{R}\right]$$

where N is the number of NaCl pairs, z the number of closest neighbors, R the distance between closest anions and cations, λ and ρ are empirical parameters describing the repulsion between closest anions and cations and α is the Madelung constant. For NaCl bulk crystal: $z = 6$, $R = 2.82$ Å, $z\lambda = 1.05$ erg, $\rho = 0.321$ Å and $\alpha = 1.747565$. The lattice parameter of an unsupported NaCl monolayer can be estimated by taking the 2D Madelung constant, which is 1.615542 [35] and by reducing z to 4. This leads to a lattice parameter of 5.36 Å ($R = 2.68$ Å).

References

[1] Yuasa S and Djayaprawira D D 2007 *J. Phys. D: Appl. Phys.* **40** R337–54
[2] Pacchioni G and Valeri S (ed) 2012 *Oxide Ultrathin Films* (New York: Wiley)
[3] Nilius N 2009 *Surf. Sci. Rep.* **64** 595–659
[4] Vassent J L, Marty A, Gilles B and Chatillon C 2000 *J. Cryst. Growth* **219** 434–43
[5] Vassent J L, Marty A, Gilles B and Chatillon C 2000 *J. Cryst. Growth* **219** 444–50
[6] Kolodziej J J, Such B, Czuba P, Krok F, Piatkowski P and Szymonski M 2002 *Surf. Sci.* **506** 12–22
[7] Vlaic P 2010 *J. Magn. Magn. Mater.* **322** 1438–14427
[8] Nakazumi M, Yoshioka D, Yanagihara H, Kita E and Koyano T 2007 *Japan. J. Appl. Phys.* **46** 6618–20
[9] Le Moal E, Müller M, Bauer O and Sokolowski M 2009 *Surf. Sci.* **603** 2434–44
[10] Parihar S S, Meyerheim H L, Mohseni K, Ostanin S, Ernst A, Jedrecy N, Felici R and Kirschner J 2010 *Phys. Rev.* B **81** 075428
[11] Tange A, Gao C, Wulfhekel W and Kirschner J 2010 *Phys. Rev.* B **81** 220404
[12] Cattoni A, Petti D, Brivio S, Cantoni M, Bertacco R and Ciccacci F 2009 *Phys. Rev.* B **80** 104437
[13] Gardner R N 1978 *J. Cryst. Growth* **43** 425–32
[14] Sadewasser S and Lux-Steiner M 2003 *Phys. Rev. Lett.* **91** 266101
[15] Prada S, Martinez U and Pacchioni G 2008 *Phys. Rev.* B **78** 235423
[16] Chang C-Y, Li H-D, Tsay S-F, Chang S-H and Lin D-S 2012 *J. Phys. Chem.* C **116** 11526–38
[17] Pivetta M, Patthey F, Stengel M, Baldereschi A and Schneider W-D 2005 *Phys. Rev.* B **72** 235423
[18] Olsson F and Persson M 2003 *Surf. Sci.* **540** 172–84
[19] Maier S, Pfeiffer O, Glatzel T, Meyer E, Filleter T and Bennewitz R 2007 *Phys. Rev.* B **75** 195408
[20] Meyer G, Gross L, Mohn F and Repp J 2012 *Chimia* **66** 10–15
[21] Calloni A, Picone A, Brambilla A, Finazzi M, Duo L and Ciccacci F 2011 *Surf. Sci.* **605** 2092–6 and references therein
[22] Dai D J 1996 *J. Chem. Phys.* **104** 6338
[23] Blonski P, Kiejna A and Hafner J 2005 *Surf. Sci.* **590** 88–100
[24] Hino S and Lambert R M 1986 *Langmuir* **2** 147–50

[25] Butler W, Zhang X-G, Schulthess T and MacLaren J 2001 *Phys. Rev.* B **63** 054416
[26] Mathon J and Umerski A 2001 *Phys. Rev.* B **63** 220403(R)
[27] Yuasa S, Nagahama T, Fukushima A, Suzuki Y and Ando K 2004 *Nature Mater.* **3** 868–71
[28] Parkin S S P, Kaiser C, Panchula A, Rice P M, Hughes B, Samant M and Yang S-H 2004 *Nature Mater.* **3** 862–7
[29] Zhang X-G, Butler W and Bandyopadhyay A 2003 *Phys. Rev.* B **68** 092402
[30] Bose P, Ernst A, Mertig I and Henk J 2008 *Phys. Rev.* B **78** 092403
[31] Ke Y, Xia K and Guo H 2010 *Phys. Rev. Lett.* **105** 236801
[32] Klaua M, Ullmann D, Barthel J, Wulfhekel W, Kirschner J, Urban R, Monchesky T, Enders A, Cochran J and Heinrich B 2001 *Phys. Rev.* B **64** 134411
[33] Mather P, Read J and Buhrman R 2006 *Phys. Rev.* B **73** 205412
[34] Kittel Ch 1996 *Introduction to Solid State Physics* 7th edn (New York: Wiley) p 66
[35] Finch S R 2003 *Mathematical Constants* (Cambridge: Cambridge University Press) p 76